

CP Violation, Stability and Unitarity of the Two Higgs Doublet Model

Abdul Wahab El Kaffas* and Per Osland†

Department of Physics and Technology, University of Bergen, Postboks 7803, N-5020 Bergen, Norway

Odd Magne Ogreid‡

Bergen University College, Bergen, Norway

(Dated: November 3, 2018)

The Two-Higgs-Doublet Model is considered, in its CP-non-conserving version. It is shown quantitatively how vacuum stability and tree-level unitarity in the Higgs-Higgs-scattering sector constrain the parameter space of the model. In particular, at high values of $\tan\beta$, the model violates unitarity, unless some of the Higgs bosons are heavy. In the regime of large CP violation in the neutral-Higgs– t -quark sector, which requires $\tan\beta \lesssim 1$, the Yukawa coupling parameter space (determined by the neutral-Higgs-sector rotation matrix) is reasonably unconstrained. On the other hand, the corresponding neutral-Higgs– b -quark sector allows for large CP violation at $\tan\beta \gg 1$. However, here the model is more constrained: Significant CP violation is correlated with a considerable splitting among the two heavier Higgs bosons.

I. INTRODUCTION

The Two-Higgs-Doublet Model (2HDM) has been proposed as an extension to the Standard Model (SM), in part because it provides an additional mechanism for CP violation [1, 2, 3, 4]. Various experimental observations impose non-trivial constraints on it. For example, the $B - \bar{B}$ oscillations [5, 6, 7] and $Z \rightarrow b\bar{b}$ decay width [8] exclude low values of $\tan\beta$, whereas the $B \rightarrow X_s\gamma$ rate [9] excludes values of the charged-Higgs mass, M_{H^\pm} , below approximately 300 GeV [10]. Also, the precise measurements at LEP of the so-called ρ parameter constrain the mass splitting in the Higgs sector, and force the masses to be not too far from the Z mass scale [11]. While these individual constraints are all well-known, we are not aware of any dedicated attempt to combine them, other than those of [12, 13].

There are also theoretical consistency conditions. In particular, for vacuum stability, the potential has to be positive for large values of the fields [14, 15]. We shall furthermore require the Higgs–Higgs scattering amplitudes to satisfy perturbative unitarity [16, 17, 18]. Taken together, these constraints dramatically reduce the allowed parameter space of the model.

The unitarity conditions are traditionally phrased in terms of upper bounds on the Higgs masses [16, 19]. The present paper is devoted to a study of the vacuum stability (or positivity) and unitarity conditions. These limits will here be seen in conjunction with the CP-violating Yukawa couplings. We will study how the CP-violating couplings are constrained by the stability and unitarity constraints, for various Higgs mass scenarios. The combination with experimental constraints will be considered elsewhere.

In our parameterization of the model, we emphasize the masses and mixing angles. The latter are closely related to the Yukawa couplings, and thus somewhat more “physical” than the parameters of the potential, to which they are clearly related.

II. THE MODEL

The present study is limited to the 2HDM (II), which is defined by having one Higgs doublet (Φ_2) couple to the up-type quarks, and the other (Φ_1) to the down-type quarks [20].

We take the 2HDM potential to be parametrized as:

$$V = \frac{\lambda_1}{2}(\Phi_1^\dagger\Phi_1)^2 + \frac{\lambda_2}{2}(\Phi_2^\dagger\Phi_2)^2 + \lambda_3(\Phi_1^\dagger\Phi_1)(\Phi_2^\dagger\Phi_2) + \lambda_4(\Phi_1^\dagger\Phi_2)(\Phi_2^\dagger\Phi_1) + \frac{1}{2} \left[\lambda_5(\Phi_1^\dagger\Phi_2)^2 + \text{h.c.} \right] - \frac{1}{2} \left\{ m_{11}^2(\Phi_1^\dagger\Phi_1) + \left[m_{12}^2(\Phi_1^\dagger\Phi_2) + \text{h.c.} \right] + m_{22}^2(\Phi_2^\dagger\Phi_2) \right\} \quad (2.1)$$

Thus, the Z_2 symmetry will be respected by the quartic terms, and Flavour-Changing Neutral Currents are constrained [21]. We shall refer to this model (without the λ_6 and λ_7 terms) as the 2HDM₅. The more general model, with also λ_6 and λ_7 couplings, will be discussed elsewhere.

We allow for CP violation, i.e., λ_5 and m_{12}^2 may be complex. All three neutral states will then mix,

$$R\mathcal{M}^2R^T = \mathcal{M}_{\text{diag}}^2 = \text{diag}(M_1^2, M_2^2, M_3^2), \quad (2.2)$$

where \mathcal{M}^2 is determined from second derivatives of the above potential. The 3×3 mixing matrix R governing the neutral sector will be parametrized in terms of the angles α_1 , α_2 and α_3 as in [4, 22]:

$$R = \begin{pmatrix} c_1 c_2 & s_1 c_2 & s_2 \\ -(c_1 s_2 s_3 + s_1 c_3) & c_1 c_3 - s_1 s_2 s_3 & c_2 s_3 \\ -c_1 s_2 c_3 + s_1 s_3 & -(c_1 s_3 + s_1 s_2 c_3) & c_2 c_3 \end{pmatrix} \quad (2.3)$$

*awkaffas@ift.uib.no

†per.osland@ift.uib.no

‡omo@hib.no

where $c_1 = \cos \alpha_1$, $s_1 = \sin \alpha_1$, etc., and

$$-\frac{\pi}{2} < \alpha_1 \leq \frac{\pi}{2}, \quad -\frac{\pi}{2} < \alpha_2 \leq \frac{\pi}{2}, \quad 0 \leq \alpha_3 \leq \frac{\pi}{2}. \quad (2.4)$$

(In ref. [22], the angles are denoted as $\tilde{\alpha} = \alpha_1$, $\alpha_b = \alpha_2$, $\alpha_c = \alpha_3$.) For these angular ranges, we have $c_i \geq 0$, $s_3 \geq 0$, whereas s_1 and s_2 may be either positive or negative. We will use the terminology ‘‘general 2HDM’’ as a reminder that CP violation is allowed.

With all three masses different, there are three limits of *no* CP violation, i.e., with two Higgs bosons that are CP even and one that is odd. The three limits are [15]:

$$\begin{aligned} H_1 \text{ odd: } & \alpha_2 \simeq \pm\pi/2, \alpha_1, \alpha_3 \text{ arbitrary,} \\ H_2 \text{ odd: } & \alpha_2 = 0, \alpha_3 = \pi/2, \alpha_1 \text{ arbitrary,} \\ H_3 \text{ odd: } & \alpha_2 = \alpha_3 = 0, \alpha_1 \text{ arbitrary.} \end{aligned} \quad (2.5)$$

These limits of no CP-violation are indicated in Fig. 1. (For future reference, we display in Fig. 1 the full range $-\pi/2 < \alpha_3 \leq \pi/2$, as is required for the general case of non-zero λ_6 and λ_7 .)

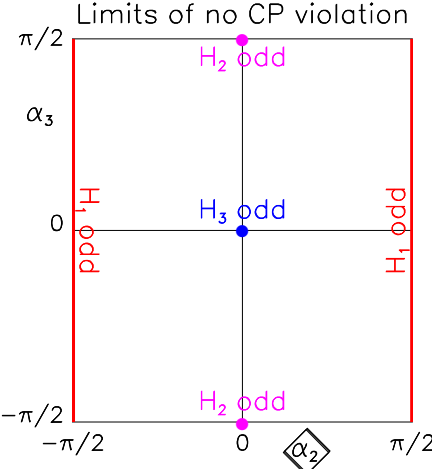


FIG. 1: Limits of no CP-violation shown in the α_2 – α_3 plane, with the CP-odd Higgs boson identified.

In the general CP-non-conserving case, the neutral sector is conveniently described by these three mixing angles, together with two masses (M_1, M_2), $\tan \beta$ and the parameter $\mu^2 = \text{Re } m_{12}^2 / (2 \cos \beta \sin \beta)$. In fact, since the Yukawa couplings are compactly expressed in terms of these rotation matrix elements,

$$\begin{aligned} H_j b \bar{b} : & \frac{1}{\cos \beta} [R_{j1} - i \gamma_5 \sin \beta R_{j3}], \\ H_j t \bar{t} : & \frac{1}{\sin \beta} [R_{j2} - i \gamma_5 \cos \beta R_{j3}], \end{aligned} \quad (2.6)$$

the angles provide a rather physical way to parametrize the model.

From Eq. (2.2), it follows that

$$(\mathcal{M}^2)_{ij} = \sum_k R_{ki} M_k^2 R_{kj}. \quad (2.7)$$

In the general CP-non-conserving case, both $(\mathcal{M}^2)_{13}$ and $(\mathcal{M}^2)_{23}$ will be non-zero. In fact, they are related by

$$(\mathcal{M}^2)_{13} = \tan \beta (\mathcal{M}^2)_{23}. \quad (2.8)$$

From these two equations, (2.7) and (2.8), we can determine M_3 from M_1, M_2 , the angles $\boldsymbol{\alpha} = (\alpha_1, \alpha_2, \alpha_3)$ and $\tan \beta$ [22]:

$$M_3^2 = \frac{M_1^2 R_{13} (R_{12} \tan \beta - R_{11}) + M_2^2 R_{23} (R_{22} \tan \beta - R_{21})}{R_{33} (R_{31} - R_{32} \tan \beta)} \quad (2.9)$$

where we impose $M_1 \leq M_2 \leq M_3$.

III. EXTRACTING THE λ

As discussed above, in the 2HDM₅, with $\text{Im } \lambda_5 \neq 0$, the two masses M_1 and M_2 will together with $\boldsymbol{\alpha}$ and $\tan \beta$ determine M_3 . Providing also M_{H^\pm} and μ^2 , all the λ ’s are determined as follows. Since the left-hand side of (2.7) can be expressed in terms of the parameters of the potential (see, for example, [15]), we can solve these equations and obtain the λ ’s in terms of the rotation matrix, the neutral mass eigenvalues, μ^2 and M_{H^\pm} :

$$\begin{aligned} \lambda_1 = & \frac{1}{c_\beta^2 v^2} [c_1^2 c_2^2 M_1^2 + (c_1 s_2 s_3 + s_1 c_3)^2 M_2^2 \\ & + (c_1 s_2 c_3 - s_1 s_3)^2 M_3^2 - s_\beta^2 \mu^2], \end{aligned} \quad (3.1)$$

$$\begin{aligned} \lambda_2 = & \frac{1}{s_\beta^2 v^2} [s_1^2 c_2^2 M_1^2 + (c_1 c_3 - s_1 s_2 s_3)^2 M_2^2 \\ & + (c_1 s_3 + s_1 s_2 c_3)^2 M_3^2 - c_\beta^2 \mu^2], \end{aligned} \quad (3.2)$$

$$\begin{aligned} \lambda_3 = & \frac{1}{c_\beta s_\beta v^2} \{c_1 s_1 [c_2^2 M_1^2 + (s_2^2 s_3^2 - c_3^2) M_2^2 \\ & + (s_2^2 c_3^2 - s_3^2) M_3^2] + s_2 c_3 s_3 (c_1^2 - s_1^2) (M_3^2 - M_2^2)\} \\ & + \frac{1}{v^2} [2 M_{H^\pm}^2 - \mu^2], \end{aligned} \quad (3.3)$$

$$\lambda_4 = \frac{1}{v^2} [s_2^2 M_1^2 + c_2^2 s_3^2 M_2^2 + c_2^2 c_3^2 M_3^2 + \mu^2 - 2 M_{H^\pm}^2], \quad (3.4)$$

$$\text{Re } \lambda_5 = \frac{1}{v^2} [-s_2^2 M_1^2 - c_2^2 s_3^2 M_2^2 - c_2^2 c_3^2 M_3^2 + \mu^2], \quad (3.5)$$

$$\begin{aligned} \text{Im } \lambda_5 = & \frac{-1}{c_\beta s_\beta v^2} \{c_\beta [c_1 c_2 s_2 M_1^2 - c_2 s_3 (c_1 s_2 s_3 + s_1 c_3) M_2^2 \\ & + c_2 c_3 (s_1 s_3 - c_1 s_2 c_3) M_3^2] + s_\beta [s_1 c_2 s_2 M_1^2 \\ & + c_2 s_3 (c_1 c_3 - s_1 s_2 s_3) M_2^2 - c_2 c_3 (c_1 s_3 + s_1 s_2 c_3) M_3^2]\}, \end{aligned} \quad (3.6)$$

where $c_\beta = \cos \beta$, $s_\beta = \sin \beta$.

While M_3^2 is given in terms of M_1^2 , M_2^2 , R and $\tan \beta$ by Eq. (2.9), it is more transparent not to substitute for M_3^2 in these expressions (3.1)–(3.6). These equations are the analogues of those of [23] for the CP-conserving 2HDM₅.

A. Large values of μ^2

At large $\mu^2 \gg M_3^2$, it is seen from (3.1) and (3.2) that λ_1 and λ_2 will eventually turn negative. This would violate stability and the model would break down. Thus, for fixed Higgs masses, there is an upper limit to μ^2 .

B. Large values of $\tan \beta$

According to the constraints of unitarity, reviewed in Sec. IV C, the couplings λ_1 , λ_2 and $|\lambda_3|$ cannot be too large. At large values of $\tan \beta$, where $c_\beta \equiv \cos \beta \rightarrow 0$, the coefficients in Eq. (3.1) multiplying M_2^2 and M_3^2 will hence be constrained. When μ^2 is small, these coefficients must be small. This requires $|s_1|$ and $|s_2|$ both to be small. Otherwise, when μ^2 is relevant, the terms proportional to M_2^2 and M_3^2 must balance against the μ^2 -term.

IV. POSITIVITY AND UNITARITY

We shall project the constraints of positivity and unitarity onto the $\tan \beta$ - M_{H^\pm} plane. Such a projection of information from a six-dimensional space onto a point in the $\tan \beta$ - M_{H^\pm} plane can be done in a variety of ways, all of which will lead to some loss of information. However, we feel that this loss of detailed information can be compensated for by the “overview” obtained by the following procedure:

1. Pick a set of neutral-Higgs-boson masses, (M_1, M_2) together with μ^2 .
2. Scan an $N = n_1 \times n_2 \times n_3$ grid in the $(\alpha_1, \alpha_2, \alpha_3)$ space, and count the number j of these points that give a viable model. (Alternatively, one could scan over N random points in this space.)
3. The ratio

$$Q = j/N, \quad 0 \leq Q \leq 1, \quad (4.1)$$

is then a figure of merit, a measure of “how allowed” the point is, in the $\tan \beta$ - M_{H^\pm} plane. If $Q = 0$, no sampled point in the $\alpha = (\alpha_1, \alpha_2, \alpha_3)$ space is allowed. Similarly, if $Q = 1$, they are all allowed. An alternative measure

$$Q_+ = j/N_+, \quad Q_+ \geq Q, \quad (4.2)$$

counts in the denominator only those points N_+ for which positivity is satisfied.

Of course the 2HDM, if realized in nature, would only exist at *one* point in this parameter space. However, we think the above quantities Q and Q_+ give meaningful measures of how “likely” different parameters are.

A. Reference masses

We shall impose the conditions of positivity and unitarity on the model, for the different “reference” mass sets given in Table I (and variations around these). For each of these mass sets we scan the model properties in the α space. From these reference masses, some trends will emerge, allowing us to draw more general conclusions.

Name	M_1 [GeV]	M_2 [GeV]	μ^2 [GeV] ²
“100-300”	100	300	$0 [\pm(200)^2]$
“150-300”	150	300	$0 [\pm(200)^2]$
“100-500”	100	500	$0 [\pm(200)^2]$
“150-500”	150	500	$0 [\pm(200)^2]$

TABLE I: Reference masses.

These masses are inspired by the indication from LEP that there is a relatively light Higgs boson [24], here denoted H_1 . The others, H_2 and H_3 , are then presumably more massive, and do not directly affect the LEP phenomenology. As an alternative, we shall also briefly consider the case of *two* light Higgs bosons, with the third one considerably more massive (see Sec. IX).

B. Stability

Let us first explore the effect of imposing vacuum stability, or positivity. The positivity conditions can be formulated as (for a general discussion, see Appendix A of [15]):

$$\begin{aligned} \lambda_1 &> 0, & \lambda_2 &> 0, \\ \lambda_3 + \min[0, \lambda_4 - |\lambda_5|] &> -\sqrt{\lambda_1 \lambda_2}. \end{aligned} \quad (4.3)$$

Actually, we will use the notion “positivity” to include also the non-trivial conditions $M_3^2 > 0$ and $M_2 \leq M_3$ [see Eq. (2.9)]. We scan the α parameter space as discussed above, and show in Table II the fraction of parameter points that satisfy “positivity”, as defined above.

μ^2	$-(200 \text{ GeV})^2$	0	$(200 \text{ GeV})^2$
“100-300”	30.8–31.0%	30.8–31.0%	24.0–28.0%
“150-300”	30.8–31.0%	30.8–31.0%	26.2–31.0%
“100-500”	30.8–31.0%	30.8–31.0%	27.3–29.7%
“150-500”	30.8–31.0%	30.8–31.0%	28.8–31.0%

TABLE II: Percentage Q of points in α space for which positivity is satisfied.

We shall henceforth refer to the set of points in the α space where positivity is satisfied, as α_+ . The fraction Q of points in the α space for which positivity is satisfied, is around 30%. (The range given indicates the lowest and highest values found when scanning over $0.5 \leq \tan \beta \leq 50$ and $200 \text{ GeV} \leq M_{H^\pm} \leq 700 \text{ GeV}$.) We note that an upper bound for this fraction is 50%. This comes about

from the fact that for a given value of $\beta + \alpha_1$, in the 2HDM₅, only positive or only negative values of α_2 are allowed, not both [22]. Thus, with $0 \leq \alpha_3 \leq \pi/2$, the sign of α_2 will be given by that of $\beta + \alpha_1$:

$$\begin{aligned} 0 < \beta + \alpha_1 < \frac{1}{2}\pi : \quad & \alpha_2 \alpha_3 > 0, \\ -\frac{1}{2}\pi < \beta + \alpha_1 < 0 : \quad & \alpha_2 \alpha_3 < 0. \end{aligned} \quad (4.4)$$

For small and negative values of μ^2 , “most” of the exclusion provided by the positivity constraint is already contained in the conditions $M_3^2 > 0$ and $M_3 > M_2$, without the explicit conditions (4.3) on the λ ’s. The conditions on the λ ’s provide the additional exclusion at positive values of μ^2 that is evident in Table II.

C. Unitarity

Perturbative unitarity in the Higgs–Higgs sector imposes upper bounds on the $|\lambda_i|$. These relations have the structure

$$\frac{1}{16\pi} \left| \sum a_i \lambda_i + \sqrt{Q(\lambda_i)} \right| \leq 1 \quad (4.5)$$

where the coefficients a_i are of $\mathcal{O}(1)$ and $Q(\lambda_i)$ is a quadratic expression [16, 17, 18]. These constraints can be expressed as upper bounds on the Higgs masses [16]. They are conveniently formulated in terms of the different weak isospin and hypercharge channels [18].

When $\mu^2 = 0$ (or negative), we see from Eq. (3.1) that λ_1 will become large when $\tan \beta \gg 1$. Thus, unitarity will at some point be violated. This is illustrated in Fig. 2, where we show in yellow where at least one point in α_+ satisfies positivity and unitarity.

V. HIGGS-MEDIATED CP VIOLATION

When the Yukawa couplings contain both a scalar and a pseudoscalar term, as in Eq. (2.6), the exchange of Higgs particles leads to CP violation via an amplitude, which for couplings to b and t -quarks is proportional to

$$Y_{\text{CP}}^b = \sum_{j=1}^3 R_{j1} R_{j3} \frac{\sin \beta}{\cos^2 \beta} f_b(M_j^2) \quad (5.1)$$

and

$$Y_{\text{CP}}^t = \sum_{j=1}^3 R_{j2} R_{j3} \frac{\cos \beta}{\sin^2 \beta} f_t(M_j^2), \quad (5.2)$$

respectively. The function $f_q(M_j^2)$ is in general some loop integral that depends on the Higgs mass M_j . This CP-violating effect is most important when the Higgs masses are not too close. Otherwise there are cancellations among different contributions, due to the orthogonality of the rotation matrix,

$$\sum_{j=1}^3 R_{j1} R_{j3} = 0, \quad \sum_{j=1}^3 R_{j2} R_{j3} = 0. \quad (5.3)$$

Also, since the functions $f_q(M^2)$ decrease for high values of M^2 , the effect tends to be larger when the lightest Higgs boson is reasonably light.

Let us therefore focus on the couplings of the lightest Higgs boson, H_1 . For maximal CP violation in the $H_1 b\bar{b}$ coupling, $R_{11} R_{13} \sin \beta / \cos^2 \beta = \frac{1}{2} \cos \alpha_1 \sin 2\alpha_2 \sin \beta / \cos^2 \beta$ must be large, requiring

$$\alpha_1 \simeq 0, \quad \alpha_2 \simeq \pm\pi/4, \quad \tan \beta \gg 1. \quad (5.4)$$

Similarly, for maximal CP violation in the $H_1 t\bar{t}$ coupling, $R_{12} R_{13} \cos \beta / \sin^2 \beta = \frac{1}{2} \sin \alpha_1 \sin 2\alpha_2 \cos \beta / \sin^2 \beta$ must be large, or

$$\alpha_1 \simeq \pm\pi/2, \quad \alpha_2 \simeq \pm\pi/4, \quad \tan \beta \lesssim 1. \quad (5.5)$$

When the two heavier Higgs bosons have a similar mass, $M = M_2 \simeq M_3$, the expression (5.2), for example, simplifies because of (5.3):

$$Y_{\text{CP}}^t \simeq R_{12} R_{13} \frac{\cos \beta}{\sin^2 \beta} [f_t(M_1^2) - f_t(M^2)]. \quad (5.6)$$

Thus, also in this case is the coupling of the lightest Higgs boson of special importance.

These two conditions (5.4) and (5.5) will be studied in the following. Common to both of them is the requirement that $\alpha_2 \simeq \pm\pi/4$. Vice versa, there is no CP violation mediated by the lightest Higgs exchange when $\alpha_2 \simeq 0$ or when $\alpha_2 \simeq \pm\pi/2$. Also, we note that the conditions (5.4) and (5.5) do not refer to α_3 .

In the case when *two* Higgs bosons are fairly light compared to the third one, by orthogonality, it will be the couplings of the heavy one that determine the amount of CP violation. For maximal CP violation in the $H_3 b\bar{b}$ coupling, $|R_{31} R_{33}| \sin \beta / \cos^2 \beta = |-c_1 s_2 c_3 + s_1 s_3| c_2 c_3 \sin \beta / \cos^2 \beta$ must then be large, requiring c_2 and c_3 to be non-zero. More explicitly, for small $|\alpha_1|$ one must have $\alpha_2 \simeq \pm\pi/4$ and $\alpha_3 \simeq 0$. At the other extreme, for $|\alpha_1| \simeq \pi/2$, one must have $\alpha_2 \simeq 0$ and $\alpha_3 \simeq \pi/4$. Similarly, for maximal CP violation in the $H_3 t\bar{t}$ coupling, $|R_{32} R_{33}| \cos \beta / \sin^2 \beta = |c_1 s_3 + s_1 s_2 c_3| c_2 c_3 \cos \beta / \sin^2 \beta$ must be large, also requiring c_2 and c_3 to be non-zero. More explicitly, for small $|\alpha_1|$ one must have $\alpha_2 \simeq 0$ and $\alpha_3 \simeq \pi/4$. At the other extreme, for $|\alpha_1| \simeq \pi/2$, one must have $\alpha_2 \simeq \pm\pi/4$ and $\alpha_3 \simeq 0$.

We shall now proceed to study to what extent these regions of large CP-violation are allowed by the stability and unitarity constraints.

VI. ALLOWED REGIONS FOR $\mu = 0$

The unitarity constraint can have a rather dramatic effect at “large” values of $\tan \beta$ and M_{H^\pm} . While the general constraints on the charged-Higgs sector exclude low values of $\tan \beta$ and M_{H^\pm} (see [5, 6, 7, 8, 9, 10, 25, 26]), the constraints of unitarity exclude high values of these same parameters. Only some region in the middle remains not excluded. For $(M_1, M_2) = (100, 300)$ GeV

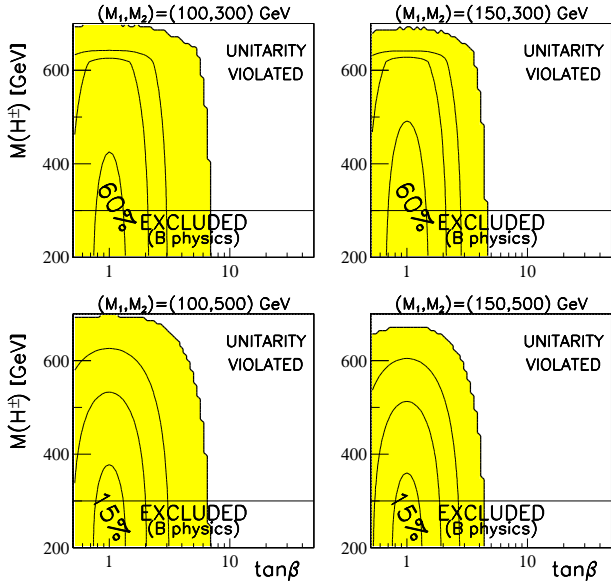


FIG. 2: Percentage of points Q_+ in the α_+ space that satisfy unitarity. Four sets of (M_1, M_2) values are considered, as indicated. All panels: $\mu^2 = 0$. Yellow region: $Q_+ > 0$ (positivity and unitarity satisfied). The contours show $Q_+ = 0, 20\%, 40\%$ and 60% (upper panels) and $0, 5\%, 10\%$ and 15% (lower panels). The line at $M_{H^\pm} = 300$ GeV indicates roughly what is excluded by the $b \rightarrow s\gamma$ constraint [10].

and $\mu = 0$ [see Fig. 2], unitarity excludes everything above $\tan\beta \sim 7$ (for any value of M_{H^\pm}), and above $M_{H^\pm} \sim 700$ GeV (for any value of $\tan\beta$).

For $M_2 = 300$ GeV, the percentage of points in α_+ space for which unitarity is satisfied, reaches (at low $\tan\beta$ and low M_{H^\pm}) beyond 60%, whereas for $M_2 = 500$ GeV, it only reaches values close to 20%.

The domains in which solutions exist ($Q_+ > 0$) depend on μ^2 : For negative values of μ^2 , the region typically shrinks to lower values of $\tan\beta$, for positive values of μ^2 it extends to larger values of $\tan\beta$ (see next section). However, the maximum values of Q_+ (at low values of $\tan\beta$), are little changed.

As discussed in Sect. III B, for large values of $\tan\beta$, the allowed solutions get constrained to a region of $|\alpha_1|$ and $|\alpha_2|$ both small. This is illustrated in Fig. 3, where we show regions of allowed α_1 and α_2 , for $\tan\beta < 5$ (lower part) and $5 < \tan\beta < 10$ (upper part). The masses considered are $(M_1, M_2) = (100, 300)$ GeV and $(100, 500)$ GeV. No allowed solutions were found for $\tan\beta \gtrsim 7$. As M_2 is increased from 300 GeV to 500 GeV, the allowed region shrinks.

As discussed in Sec. V, the Yukawa couplings of the lightest Higgs particle to b and t quarks is large for $\tan\beta$ low or high, with $|\alpha_1| \simeq \pi/2$ or 0, respectively, and $|\alpha_2| \simeq \pi/4$ in both cases. These regions will be referred to as “regions of major CP violation” and are indicated by boxes labeled “ b ” and “ t ” in Fig. 3. We note that the boxes labeled “ b ” are empty, the model does not give

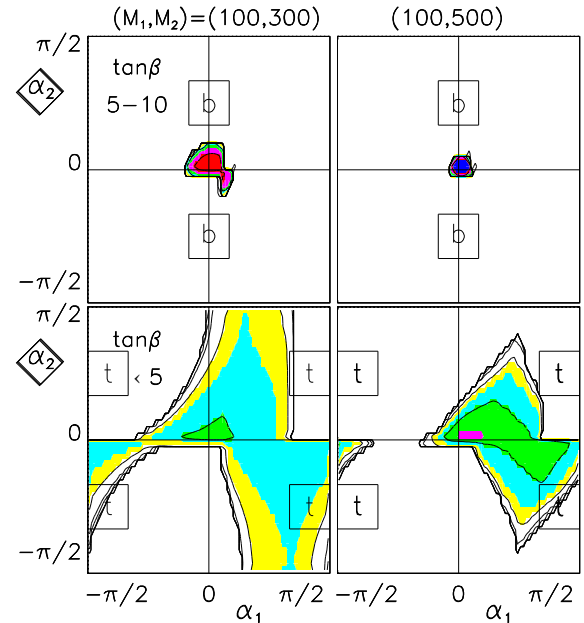


FIG. 3: Allowed regions in the α_1 – α_2 plane, for $(M_1, M_2) = (100, 300)$ GeV and $(100, 500)$ GeV, $\mu = 0$ and two slices in $\tan\beta$ as indicated. At higher values of $\tan\beta$ there are no allowed points (see also Fig. 2). Contours are shown at each negative power of 10, as appropriate. Yellow (light blue) indicates where the normalized distribution is higher than 10^{-4} (3×10^{-4}); green (purple) levels above 10^{-3} (3×10^{-3}); red (dark blue) is above 10^{-2} (3×10^{-2}). Regions of major CP violation are labeled “ b ” and “ t ”.

large CP violation in the bbH_1 couplings for these mass and μ parameters.

Since at high $\tan\beta$, $|\alpha_1|$ and $|\alpha_2|$ are small, M_3 will be almost degenerate with M_2 . The distribution of M_3 values is shown in Table III. It is seen that M_3 is just barely larger than M_2 , in particular for high values of $\tan\beta$ and high values of M_2 (cf. $M_2 = 500$ GeV vs. 300 GeV).

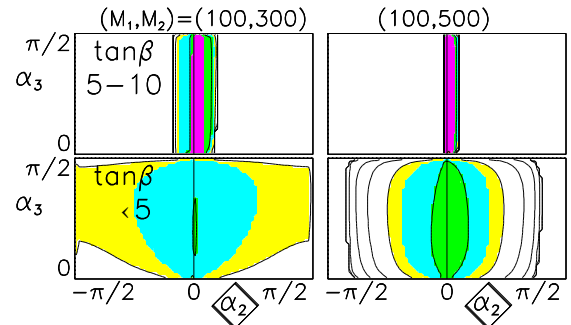


FIG. 4: Allowed regions in the α_2 – α_3 plane, for $(M_1, M_2) = (100, 300)$ GeV and $(100, 500)$ GeV, $\mu = 0$ and two slices in $\tan\beta$ as indicated. Contours and colour coding as in Fig. 3.

$(M_1, M_2) = (100, 300 [500]) \text{ GeV}$			
$\tan \beta$	$\xi < 1.1$	$1.1 < \xi < 1.5$	$1.5 < \xi$
5 – 10	94.4 [98.5]%	5.4 [1.5]%	0.2 [0.0]%
< 5	41.1 [82.5]%	50.2 [17.5]%	8.6 [0.0]%

TABLE III: Distribution of M_3 values, $\xi = M_3/M_2$. Contours and colour coding as in Fig. 3.

The distribution in α_3 , of allowed solutions, is more spread out, as shown in Fig. 4.

At large values of $\tan \beta$ it turns out to be the isospin-zero, hypercharge-zero channel that is most constraining.

When $\mu^2 < 0$, the range in $\tan \beta$ is likewise limited, and the allowed regions in α_1 , α_2 and α_3 are similar to those for the $\mu^2 = 0$ case.

VII. ALLOWED REGIONS FOR $M_1 \lesssim \mu$

The large- μ case is often referred to as the decoupling limit. It has received considerable attention in the CP-conserving case [27]. Within the framework set up by our choice of input parameters, it is natural to distinguish three mass scales: M_1 , M_2 and μ . Thus, there are three cases:

- (i) $\mu < M_1 < M_2$, Sect. VI,
- (ii) $M_1 < \mu < M_2$, decoupling,
- (iii) $M_1 < M_2 < \mu$, decoupling. (7.1)

If μ is “significantly” larger than M_1 , the latter two both correspond to decoupling in the sense of Gunion and Haber [27], but from the point of view of CP violation, they can be rather different.

In these regimes of $M_1 < \mu$, it is possible to keep λ_1 and $|\lambda_3|$ within the allowed range (not too large) by carefully tuning the other parameters. For μ suitably chosen (large), no part of the $\tan \beta$ - M_{H^\pm} plane is disallowed. From an inspection of Eq. (3.1) for λ_1 , we see that $|s_1|$ and/or $|s_2|$ must be small. But they can not both be zero, unless M_1 is very close to μ . This region of small $|s_1|$ and/or $|s_2|$ will also yield solutions for λ_3 that are sufficiently small. In the following, we discuss the specific examples of $(M_1, M_2) = (100, 300) \text{ GeV}$ and $(100, 500) \text{ GeV}$, each of them for two values of μ .

A. $(M_1, M_2) = (100, 300) \text{ GeV}$

We display in Figs. 5 and 6 the allowed regions in the α_1 - α_2 and α_2 - α_3 planes, for three slices in $\tan \beta$ and two values of μ , “small” (200 GeV) and “moderate” (400 GeV). At $\tan \beta < 5$ sizable regions in α space are populated with allowed solutions, but these regions shrink significantly for $\tan \beta > 5$.

From Figs. 5 and 6, we see that for large $\tan \beta$ and increasing μ , the majority of solutions have values of α_2

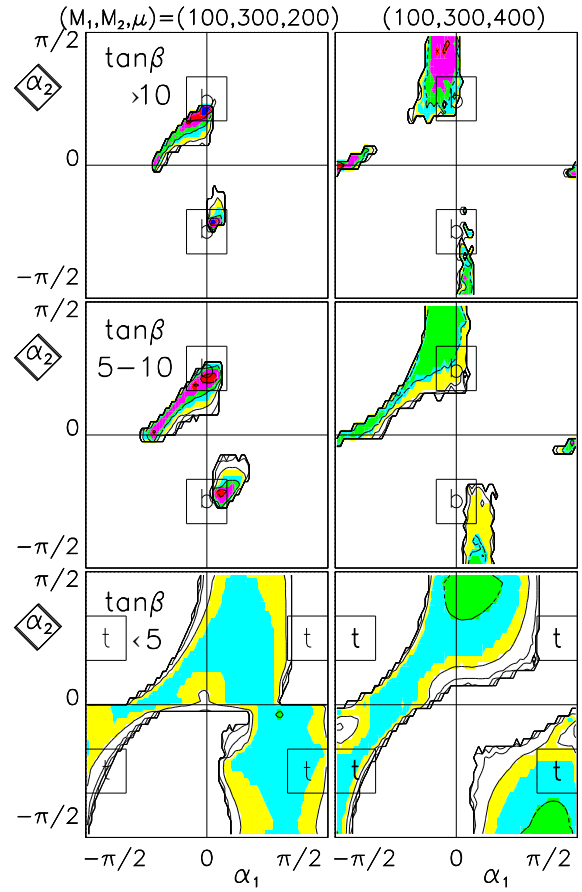


FIG. 5: Allowed regions in the α_1 - α_2 plane, for $(M_1, M_2) = (100, 300) \text{ GeV}$, $\mu = 200 \text{ GeV}$ and 400 GeV and three slices in $\tan \beta$ as indicated. Contours and colour coding as in Fig. 3. Regions of major CP violation are labeled “b” and “t”.

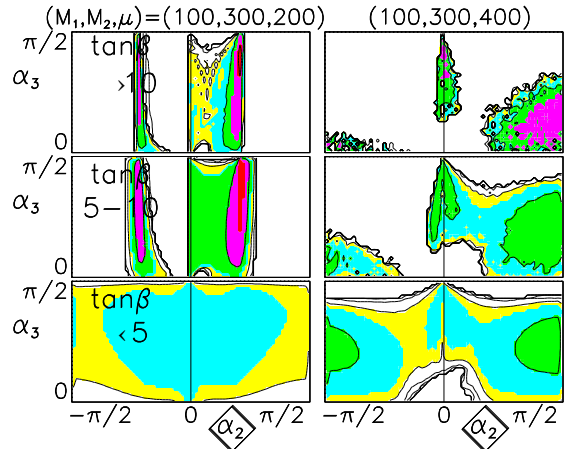


FIG. 6: Allowed regions in the α_2 - α_3 plane, for $(M_1, M_2) = (100, 300) \text{ GeV}$, $\mu = 200 \text{ GeV}$ and 400 GeV and three slices in $\tan \beta$ as indicated. Contours and colour coding as in Fig. 3.

that move away from 0 towards $\pi/2$ (where CP is conserved, see Fig. 1). In this case of increasing μ , M_3 will also increase, and the last two terms of (3.1) must compensate each other. In distinction from the case of $\mu = 0$, $|s_1|$ and $|s_2|$ can then not both be small, one of them will approach unity, as seen from Fig. 5. According to (4.3), λ_3 can not be too large and negative. From Eq. (3.3), this means that either s_1 (i.e., α_1) or s_2 (i.e., α_2) must be large and positive, as seen in Figs. 5 and 6.

There will for large values of $\tan\beta$ be a range of μ -values for which the allowed solutions accumulate around $\alpha_2 \simeq \pm\pi/4$. In these regions, the CP-violation in the $H_1 b\bar{b}$ -coupling will be considerable.

The distribution of M_3 -values is shown in Table IV. Here, we note that for $M_1 < \mu < M_2$, the values of M_3 are rather low (close to M_2), whereas for $M_2 < \mu$ they tend to be considerably higher.

$(M_1, M_2, \mu) = (100, 300, 200 [400])$ GeV

$\tan\beta$	$\xi < 1.1$	$1.1 < \xi < 1.5$	$1.5 < \xi$
> 10	58.6 [0.0]%	40.0 [70.4]%	1.4 [29.6]%
$5 - 10$	41.8 [0.0]%	55.3 [44.2]%	3.0 [55.8]%
< 5	29.7 [0.0]%	56.1 [13.1]%	14.2 [86.9]%

TABLE IV: Distribution of M_3 values, $\xi = M_3/M_2$.

B. $(M_1, M_2) = (100, 500)$ GeV

For this case of “large” M_2 , we display in Fig. 7 the allowed regions in the α_1 - α_2 plane, for three slices in $\tan\beta$ and two values of μ , 200 GeV and 600 GeV.

In this region of large M_2 , we note that at high values of $\tan\beta$, the allowed regions in α_1 get constrained to values around $\alpha_1 \simeq 0$ or $\alpha_1 \simeq \pm\pi/2$ with $|\alpha_2|$ increasing with μ from 0 to $\pi/2$. (We recall that the $\alpha_2 \rightarrow \pi/2$ limit represents the case when the lightest Higgs particle, H_1 , is odd, and there is no CP violation.) It follows from Eq. (2.9) that when $|\alpha_1|$ and $|\alpha_2|$ are both small, M_3 is close to M_2 . Furthermore, it follows from (3.1) that in this limit, we have

$$\lambda_1 \simeq \frac{1}{c_\beta^2 v^2} [\frac{1}{2} M_1^2 + \frac{1}{2} s_3^2 M_2^2 + \frac{1}{2} c_3^2 M_3^2 - s_\beta^2 \mu^2]. \quad (7.2)$$

This should not get too large, in order not to spoil unitarity. Since M_2 and M_3 are comparable in this case, the distribution in α_3 becomes wide. This is analogous to the situation shown in Fig. 6, left panel.

$(M_1, M_2, \mu) = (100, 500, 200/[600])$ GeV

$\tan\beta$	$\xi < 1.1$	$1.1 < \xi < 1.5$	$1.5 < \xi$
> 10	93.7 [0.0]%	6.3 [94.8]%	0.0 [5.2]%
$5 - 10$	84.9 [0.0]%	15.1 [93.7]%	0.0 [6.3]%
< 5	74.1 [0.0]%	25.9 [91.5]%	0.0 [8.5]%

TABLE V: Distribution of M_3 values, $\xi = M_3/M_2$.

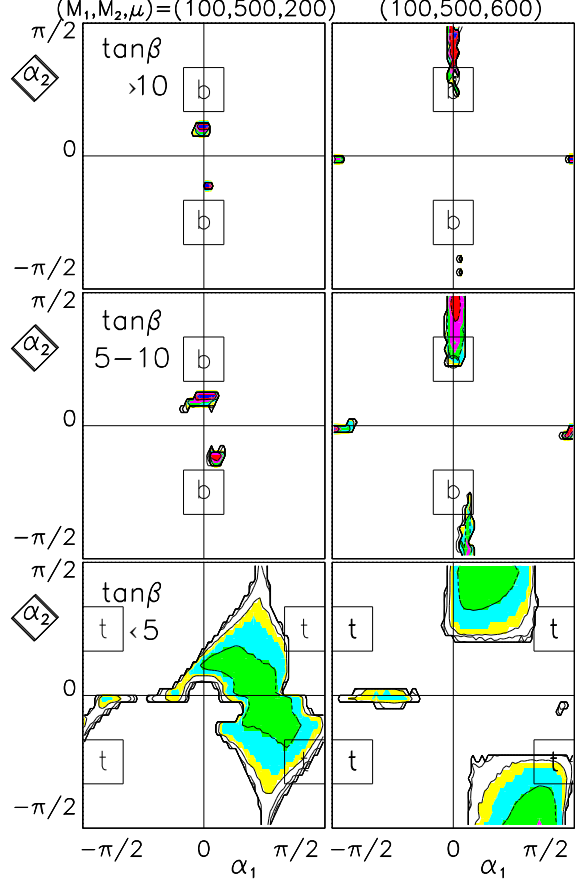


FIG. 7: Allowed regions in the α_1 - α_2 plane, for $(M_1, M_2) = (100, 500)$ GeV, $\mu = 200$ GeV and 400 GeV and three slices in $\tan\beta$ as indicated. Regions of major CP violation are labeled “b” and “t”.

As discussed above, when $\tan\beta \gg 1$, the allowed range of M_3 values get squeezed to a narrow band just above M_2 . This is illustrated in Table V.

When μ increases still, the situation becomes reminiscent of that shown in Fig. 5, right part. The majority of allowed solutions move towards $\alpha_1 \simeq 0$ and $\alpha_2 \simeq \pm\pi/2$, with small islands of additional solutions at $\alpha_1 \simeq \pm\pi/2$ and $\alpha_2 \simeq 0$.

VIII. CP-CONSERVING LIMITS

In addition to the general criteria for limits of no CP violation given in Eq. (2.5) and Fig. 1, there are important limits in which there is no CP violation in the Yukawa couplings involving the *lightest* Higgs boson: $b\bar{b}H_1$ and $t\bar{t}H_1$.

A. CP-conserving $b\bar{b}H_1$ coupling

The regions of CP-invariant $b\bar{b}H_1$ coupling require *either* $R_{11} \simeq 0$ (implying $\alpha_1 \simeq \pm\pi/2$ and/or $\alpha_2 \simeq \pm\pi/2$) *or* $R_{13} \simeq 0$ (implying $\alpha_2 \simeq 0$). These limits are shown in Fig. 8. We see from Figs. 3, 5 and 7 that both these categories of CP-conserving regions exist for $\mu = 0$ as well as for $\mu > 0$.

B. CP-conserving $t\bar{t}H_1$ coupling

The regions of CP-invariant $t\bar{t}H_1$ coupling require *either* $R_{12} \simeq 0$ (implying $\alpha_1 \simeq 0$ and/or $\alpha_2 \simeq \pm\pi/2$) *or* $R_{13} \simeq 0$ (implying $\alpha_2 \simeq 0$). These limits are shown in Fig. 8. We see from the lower panels in Figs. 3, 5 and 7 that such regions exist for $\mu = 0$ as well as for $\mu > 0$.

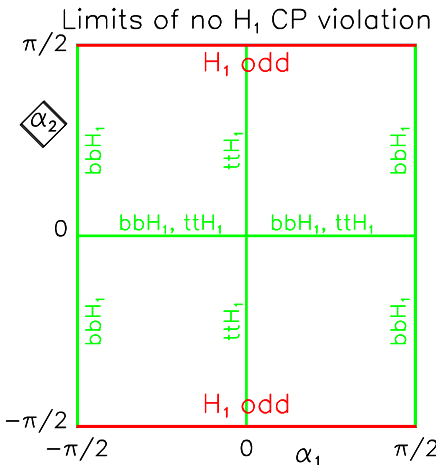


FIG. 8: Limits of no CP-violation in the $b\bar{b}H_1$ and $t\bar{t}H_1$ Yukawa couplings, shown in the α_1 – α_2 plane. Also indicated, are the limits of H_1 odd, where there is no CP violation involving *any* of the three Higgs bosons.

IX. TWO LIGHT HIGGS BOSONS

In this section, we report on some results obtained with $M_1 = 100$ GeV and $M_2 = 150$ GeV (or 200 GeV). There are two questions: (1) Which parts of the $\tan\beta$ – M_{H^\pm} plane are populated by allowed solutions, and (2) to what extent do such models provide CP violation? Concerning the latter question, we recall that two light Higgs bosons will to some extent act coherently, with Yukawa strength proportional (by orthogonality) to that of the heaviest one, H_3 .

A. $\mu = 0$

This case is similar to the case discussed in Sec. VI in the sense that for $\mu = 0$ (or small), there is an upper limit to $\tan\beta$. That limit is lifted as μ is increased. At low $\tan\beta$ and $\mu = 0$, for example, the majority of solutions fall in the domain of small $|\alpha_1|$, small $|\alpha_2|$, and large α_3 , as is required for significant CP violation in the t -quark sector (see the discussion at the end of Sec. V). At larger values of $\tan\beta$ (and $\mu = 0$), the solutions still populate the small $|\alpha_1|$, small $|\alpha_2|$ region, which is unfavorable for CP violation in the b -quark sector.

B. $M_2 < \mu$

Let us first consider the case of $\tan\beta = \mathcal{O}(1)$. As compared with the case $\mu = 0$, when μ increases, $|\alpha_1|$, $|\alpha_2|$ and $|\alpha_3|$ all tend to move towards larger values, $|\alpha_1| \rightarrow \pi/2$, $|\alpha_2| \rightarrow \pi/2$, $\alpha_3 \rightarrow \pi/2$. This limit does not satisfy the conditions for major CP violation in the t -quark sector. At larger values of $\tan\beta$, the solutions move towards intermediate and negative values of α_1 , intermediate values of α_2 , and intermediate values of α_3 , which is a favorable parameter region for CP violation in the b -quark sector.

X. CONCLUDING REMARKS

We have made a survey of parameter regions of large CP violation in the Two Higgs Doublet Model. Because of the many independent model parameters, it is difficult to extract a simple picture. For the admittedly limited set of parameters studied, it was found that considerable CP violation can easily occur in the $t\bar{t}H_1$ coupling at low values of $\tan\beta$. In order to have significant CP violation in the $b\bar{b}H_1$ coupling, on the other hand, it appears necessary to have a large mass splitting among the two heavier Higgs bosons, H_2 and H_3 .

Acknowledgment

It is a pleasure to thank O. Brein, M. Krawczyk and A. Pilaftsis for very useful discussions. This research has been supported in part by the Mission Department of Egypt and by the Research Council of Norway.

[1] T. D. Lee, Phys. Rev. D **8**, 1226 (1973).
[2] S. Weinberg, Phys. Rev. Lett. **37**, 657 (1976).

[3] G. C. Branco and M. N. Rebelo, Phys. Lett. B **160**, 117 (1985); J. Liu and L. Wolfenstein, Nucl. Phys. B **289**,

1 (1987); S. Weinberg, Phys. Rev. D **42**, 860 (1990); Y. L. Wu and L. Wolfenstein, Phys. Rev. Lett. **73**, 1762 (1994) [arXiv:hep-ph/9409421].

[4] E. Accomando *et al.*, arXiv:hep-ph/0608079.

[5] L. F. Abbott, P. Sikivie and M. B. Wise, Phys. Rev. D **21**, 1393 (1980); T. Inami and C. S. Lim, Prog. Theor. Phys. **65**, 297 (1981) [Erratum-ibid. **65**, 1772 (1981)]; G. G. Athanasiu, P. J. Franzini and F. J. Gilman, Phys. Rev. D **32**, 3010 (1985); S. L. Glashow and E. Jenkins, Phys. Lett. B **196**, 233 (1987); C. Q. Geng and J. N. Ng, Phys. Rev. D **38**, 2857 (1988) [Erratum-ibid. D **41**, 1715 (1990)].

[6] J. Urban, F. Krauss, U. Jentschura and G. Soff, Nucl. Phys. B **523**, 40 (1998) [arXiv:hep-ph/9710245].

[7] P. Ball and R. Fleischer, Eur. Phys. J. C **48**, 413 (2006) [arXiv:hep-ph/0604249].

[8] A. Denner, R. J. Guth, W. Hollik and J. H. Kuhn, Z. Phys. C **51**, 695 (1991).

[9] A. J. Buras, M. Misiak, M. Munz and S. Pokorski, Nucl. Phys. B **424**, 374 (1994); [arXiv:hep-ph/9311345]. K. G. Chetyrkin, M. Misiak and M. Munz, Phys. Lett. B **400**, 206 (1997) [Erratum-ibid. B **425**, 414 (1998)] [arXiv:hep-ph/9612313]; A. J. Buras, A. Kwiatkowski and N. Pott, Phys. Lett. B **414**, 157 (1997) [Erratum-ibid. B **434**, 459 (1998)] [arXiv:hep-ph/9707482]; M. Ciuchini, G. Degrassi, P. Gambino and G. F. Giudice, Nucl. Phys. B **527**, 21 (1998) [arXiv:hep-ph/9710335]; H. M. Asatrian, C. Greub, A. Hovhannisyan, T. Hurth and V. Poghosyan, Phys. Lett. B **619**, 322 (2005) [arXiv:hep-ph/0505068]; P. Gambino and M. Misiak, Nucl. Phys. B **611**, 338 (2001) [arXiv:hep-ph/0104034].

[10] M. Misiak *et al.*, arXiv:hep-ph/0609232.

[11] S. Bertolini, Nucl. Phys. B **272**, 77 (1986).

[12] A. K. Grant, Phys. Rev. D **51**, 207 (1995) [arXiv:hep-ph/9410267].

[13] K. Cheung and O. C. W. Kong, Phys. Rev. D **68**, 053003 (2003) [arXiv:hep-ph/0302111].

[14] N. G. Deshpande and E. Ma, Phys. Rev. D **18**, 2574 (1978); S. Nie and M. Sher, Phys. Lett. B **449**, 89 (1999) [arXiv:hep-ph/9811234]; S. Kanemura, T. Kasai and Y. Okada, Phys. Lett. B **471**, 182 (1999) [arXiv:hep-ph/9903289].

[15] A. W. El Kaffas, W. Khater, O. M. Ogreid and P. Osland, arXiv:hep-ph/0605142.

[16] S. Kanemura, T. Kubota and E. Takasugi, Phys. Lett. B **313**, 155 (1993) [arXiv:hep-ph/9303263].

[17] A. G. Akeroyd, A. Arhrib and E. M. Naimi, Phys. Lett. B **490**, 119 (2000) [arXiv:hep-ph/0006035]; A. Arhrib, arXiv:hep-ph/0012353.

[18] I. F. Ginzburg and I. P. Ivanov, arXiv:hep-ph/0312374; Phys. Rev. D **72**, 115010 (2005) [arXiv:hep-ph/0508020].

[19] B. W. Lee, C. Quigg and H. B. Thacker, Phys. Rev. D **16**, 1519 (1977).

[20] J.F. Gunion, H.E. Haber, G. Kane, S. Dawson, *The Higgs Hunter's Guide* (Addison-Wesley, Reading, 1990).

[21] S. L. Glashow and S. Weinberg, Phys. Rev. D **15**, 1958 (1977).

[22] W. Khater and P. Osland, Nucl. Phys. B **661**, 209 (2003) [arXiv:hep-ph/0302004].

[23] R. Casalbuoni, D. Dominici, F. Feruglio and R. Gatto, Nucl. Phys. B **299**, 117 (1988).

[24] [ALEPH Collaboration and DELPHI Collaboration and L3 Collaboration and OPAL Collaboration and LEP Electroweak Working Group], arXiv:hep-ex/0511027.

[25] A. Abulencia *et al.* [CDF - Run II Collaboration], Phys. Rev. Lett. **97**, 062003 (2006) [AIP Conf. Proc. **870**, 116 (2006)] [arXiv:hep-ex/0606027].

[26] W. M. Yao *et al.* [Particle Data Group], J. Phys. G **33**, 1 (2006).

[27] J. F. Gunion and H. E. Haber, Phys. Rev. D **67**, 075019 (2003) [arXiv:hep-ph/0207010].